

AD-A124 552 LASER INDUCED BUNCH LENGTHENING ON THE ACO STORAGE RING 1//  
FEL(U) STANFORD UNIV CA HIGH ENERGY PHYSICS LAB  
K E ROBINSON ET AL. SEP 82 HEPL-910 F49620-80-C-0068

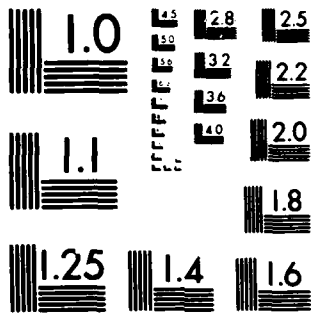
UNCLASSIFIED

F/G 20/7

NL



END  
DATE  
FILMED  
A-83  
DTIC



MICROCOPY RESOLUTION TEST CHART  
NATIONAL BUREAU OF STANDARDS-1963-A

(Submitted to IEEE  
Trans. Quant. Elect.)

Q

HEPL 910

SEPTEMBER 1982 ,

LASER INDUCED BUNCH LENGTHENING ON THE ACO STORAGE RING FEL\*

Kem Edward Robinson, David A. G. Deacon,<sup>†</sup> Michel F. Velghe<sup>‡</sup> and John M. Madey<sup>§</sup>

High Energy Physics Laboratory  
Stanford University  
Stanford, California 94305-2184



ADA 124552

DTIC FILE COPY

- \* Work supported by AFOSR F 49620-80-C-0068, DGRST 79-7-0163 and DRET 9-073.
- † Deacon Research, 3790 El Camino Real, No. 162, Palo Alto, CA 94306.
- ‡ Laboratoire de Photophysique Moléculaire, Bâtiment 210, Université de Paris-Sud, 91405, Orsay France
- § Department of Electrical Engineering, Stanford University, Stanford, CA 94305.

83 02 014 152

LASER INDUCED BUNCH LENGTHENING ON THE ACO STORAGE RING FEL+

Kem Edward Robinson  
W. W. Hansen Laboratory of Physics  
Stanford University, Stanford, CA 94305

David A. G. Deacon  
Deacon Research, 3790 El Camino Real No.162, Palo Alto, CA 94386

Michel F. Velghe  
Laboratoire de Photophysique Moléculaire, Bâtiment 210,  
Université de Paris-Sud, 91405, Orsay, France.

John M. J. Madey  
Department of Electrical Engineering,  
Stanford University, Stanford, CA 94305

ABSTRACT

Laser induced bunch lengthening has been measured on the ACO storage ring FEL. The experimental data at low current generally confirms the existing theoretical models, while the high current data is dominated by anomalous effects.

INTRODUCTION

As part of the LURE/Stanford Free Electron Laser Project at Orsay, France, we have developed a sensitive method to measure the laser induced change in the electron bunch length. This method is capable of measuring the absolute bunch with a precision of 1%, and fractional changes in electron bunch length as small as 1 part in 10<sup>4</sup>. Using this system, we have measured the steady state and time dependent laser induced bunch lengthening as a function of electron current, external laser intensity, RF cavity voltage, the undulator magnetic field, and the detection frequency. While the results that we have obtained agree with the theory in the low current region, the anomalous effects which determine the the electron bunch length and energy spread at high current can lead to a number of anomalous effects at high current, including laser-induced bunch shortening. We present in this paper a summary of the experimental procedures, and describe the basic steady state and time dependent bunch lengthening data including the dependence on the resonance energy. Additional experimental results will be dealt with in subsequent publications.

Our interest in laser induced bunch lengthening is motivated by the critical role this mechanism is believed to play in the determination of the power output and efficiency of storage ring FEL's. In a non-isochronous



Accession For	
NTIS GRA&I	<input checked="" type="checkbox"/>
DTIC TAB	<input type="checkbox"/>
Unannounced	<input type="checkbox"/>
Justification	
By _____	
Distribution/	
Availability Codes	
Avail and/or	Dist
Special	
A	<del>_____</del>

storage ring FEL, the energy spread induced by the laser is believed to set an upper limit to the laser power output and efficiency. Analyses of the mechanism have been published for the idealized SRFEL by Renieri, Elias, and others [1,3]. The experiments reported here were designed to test these theories, and to establish an experimental data base for future development of the SRFEL.

#### EXPERIMENTAL PROCEDURE

The experimental setup is shown in Figure 1. That part of experimental setup which concerns the external laser, undulator and the storage ring is similar to the one used for gain measurements on ACO [2]. An argon ion laser is coupled to the electron beam in the undulator through a mode matching telescope system and optical transport system. Synchrotron light from a bending magnet on the ACO storage ring is detected on a fast photodiode. The detector's location at the bending magnet was chosen to prevent any spurious light from the laser or undulator from reaching the photodiode. The signal from the photodiode is sent via a low dispersion coaxial cable to an AILTECH 757 RF Spectrum Analyzer. The analyzer is interfaced directly with the computer used for data acquisition for global spectrum analysis. When monitoring the bunch length changes, the analyzer is operated in the receiver mode tuned to a harmonic of the orbit frequency. The analyzer output can either be fed into a lock-in amplifier for synchronous detection at the frequency of the the laser chopper, or time averaged measurements can be made using an averaging digital oscilloscope. In all cases the detected signal is fed into the data acquisition system together with the storage ring parameters including the RF voltage, the storage ring current, and the output power of the external laser.

The synchrotron light emitted by the electrons in a bending magnet of the storage ring has the form of a series of pulses whose period is fixed by the orbit frequency, and whose shape is determined by the electron bunch shape. The fourier transform of the signal from the photodiode will be a comb spectrum whose envelope (corrected for the photodiode's frequency response) will be the fourier transform of the electron bunch shape.

Under idealized conditions, the electron pulse shape should be gaussian [4], and the fourier transform of the synchrotron light should have a gaussian envelope. The measurements on ACO confirm this model to high precision. For a typical 200psec electron bunch, the envelope of the fourier transform, corrected for photodiode frequency response, can be least-squares fit to a gaussian with an uncertainty below 2% and a mean-squared correlation exceeding 98%.

Assuming a gaussian electron bunch shape, the power spectrum  $F(\omega)$  of the photodiode output will have the form:

$$F(\omega) \propto p(\omega) e^{-\omega^2 \sigma^2 / 2}$$

where  $p(\omega)$  is the response of the measuring system,  $\sigma$  the temporal bunch length, and  $\omega$  the detection frequency. If the detection frequency is fixed and the temporal bunch length changes from  $\sigma_1$  to  $\sigma_2$ , the detected signal varies with the electron bunch length as

$$\ln \left( \frac{F_2(\omega)}{F_1(\omega)} \right) = -\frac{\omega^2}{2} \Delta\sigma^2$$

where  $\Delta\sigma^2$  is defined as  $\sigma_2^2 - \sigma_1^2$ . The fractional change in signal amplitude is determined by the absolute change in the bunch length, and scales as the square of the detection frequency. Note also that the fractional change in the detected signal is unaffected by the response of the photodiode.

Given the value of  $\log F(\omega)$  at a particular frequency, bunch length change measurements can be performed in several different ways. Steady-state measurements can be made simply by monitoring the dc component of the signal. This was the method used in the first measurements made by this system in May 1981, using the superconducting undulator originally mounted on ACO [4]. Synchronous detection can also be used, by chopping the external laser at a frequency below energy damping time of the ring, and using a lock-in detector to measure the amplitude of the resulting periodic change in  $\log F(\omega)$ . The time response of the electron beam to the chopped laser beam can be measured by recording the time-dependent waveform of  $\log F(\omega)$  on an averaging oscilloscope.

The sensitivity and precision achievable by these frequency domain measurements is superior to that achievable with the available temporal methods. While streak cameras have comparable resolution, precise absolute measurements require multiple corrections for electron transit time spread and film density. No such corrections are required in our frequency domain measurements in which transit time spread in the photodiode has no effect on the detected signal.

#### EXPERIMENTAL RESULTS

All of the bunch length measurements reported here were performed using the permanent magnet undulator which was mounted on ACO at the beginning of 1982 [5]. Measurements were performed in the low, moderate, and high current regimes. Figure 2 shows the time averaged response of the electron bunch length to the chopped external laser in the low current region (less than 1mA total average current). The parameters relevant to the bunch lengthening at the time of the experiment are shown in Table 1. Note that a fall in  $F(\omega)$  in Figure 2 signifies an increase in the bunch length.

The signal shown in Figure 2 indicates a steady state bunch lengthening of 5%. The magnitude of the bunch lengthening and the exponential response of the signal appear consistent with existing bunch lengthening models [1,3].

W

Figure 3 shows the experimental and theoretical bunch lengthening curves at low current and the spontaneous emission power at the external laser wavelength as functions of the gap between the pole faces of the permanent magnet undulator. For the permanent magnet ACO undulator, the wiggler parameter  $K$  and resonance energy  $\gamma_0$  can be computed from the gap spacing using the relations:

$$K = 8.5 \exp[-.0404 \text{ Gap(mm)}]$$

$$\gamma_0 = \left[ \frac{\lambda_0}{2\lambda} \left( 1 + \frac{K^2}{2} \right) \right]^{1/2}$$

Theoretically the bunch lengthening curve and the spontaneous emission curve should have the same functional form [2]. This prediction is also confirmed by Figure 3. Note that the maximum of the curves occur at a gap of 36.7mm which corresponds to a  $K$  of 1.93. The maximum signal shown corresponds to a bunch lengthening of 6%. The experimental curve in Figure 3 was recorded using synchronous detection.

In the moderate and high current regimes, important anomalous effects appear which are not accounted for by the simple bunch lengthening theory. These effects include space charge modifications to the RF accelerating potential, and the interactions of the electron beam with the electromagnetic modes of the vacuum cavity. The omission of these effects in the existing bunch lengthening models results in their failure as the current is raised. Figure 4 shows the response of the electron beam to the external laser at three different operating points in the moderate current regime. Figures 4a and 4b may be compared directly to Figure 2 since they have identical chopping periods. The vertical scale of figure 4a, b, and c, are 1.57, .5, and twice that of figure 2 respectively.

Note that the bunch lengthening signal in Figure 4a is  $180^\circ$  out of phase with the signal in Figure 2. This phase change is reproducible and indicates the electron bunch length was reduced by the external laser. In contrast to the electron bunch heating in Figure 2, the laser cooled the electron beam in Figure 4a.

The response of the electron beam varies as the current decays and various thresholds that are present in the anomalous bunch lengthening regime are crossed [6]. Anomalous bunch lengthening effects are seen in ACO when the average stored current exceeds 1mA. Another typical phenomena in this regime is that shown in figure 4b. Here a complicated multiple time constant structure appears in response to the laser. Figure 4c shows oscillations in the bunch length which also occur in the anomalous regime.

While the low current bunch lengthening data is consistent with existing theoretical models, the qualitative and quantitative discrepancies at high current indicate that effects present in this regime can

dramatically alter the excitation of the electrons by the laser. These results indicate that the theoretical models must be modified to include high current effects. It is possible that the observed laser-induced cooling may have significant practical implications for storage ring FEL's and in synchrotron radiation and colliding beams research where it is desirable to maximize the charge density at high current.

#### ACKNOWLEDGEMENTS

We would like to thank the other members of the LURE/Stanford FEL group for their assistance during runs and the administrative and technical staffs of LURE and the Laboratoire d'Accelérateur Lineaire at Orsay, France.

+ This work supported in part by AFOSR under contract F 49620-80-C-0068, the DGRST under contract 79-7-0163, and the DRET under contract 9-073.

#### REFERENCES

- [1] A. Renieri, IEEE Trans. Nucl. Sci. 26 (1979) 3827-9 2. L. R. Elias, J. M. J. Madey, and T. I. Smith, Appl. Phys. 23 (1980) 9. C. Pellegrini, IEEE Trans. Nucl. Sci. NS-26, (1979), No. 3, June 4.
- [2] D. A. G. Deacon, J. M. J. Madey, K. E. Robinson, C. Bazin, M. Billardon, P. Elleaume, Y. Farge, J. M. Ortega, Y. Petroff and M. F. Velghe; IEEE Trans. Nucl. Sci. NS-28, 3142 (1981).
- [3] M. Sands, "The Physics of Electron Storage Rings: An Introduction", SLAC report No. 121 (1965), Stanford Linear Accelerator Center, Stanford, CA 94305.
- [4] C. Bazin, M. Billardon, D. A. G. Deacon, P. Elleaume, Y. Farge, J. M. J. Madey, J. M. Ortega, Y. Petroff, K. E. Robinson, M. Velghe; in "Physics of Quantum Electronics" Vol. 8, p. 89, eds: S. F. Jacobs, G. T. Moore, M. S. Pilloff, M. Sargent III, M. O. Scully, and R. Spitzer (Addison-Wesley) 1982.
- [5] J. M. Ortega, C. Bazin, D. A. G. Deacon, C. Depautex, P. Elleaume, "The Realization of the Permanent Magnet Undulator NOEL", To be published in Nucl. Instr. and Meth.
- [6] P. B. Wilson, R. Servranckx, A. P. Sabarsky, J. Gareyte, G. E. Fischer, A. W. Chao, IEEE Trans. Nucl. Sci. NS-24 (1977), 1211-1214.

TABLE I  
EXPERIMENTAL PARAMETERS

Electron Energy	E	238Mev
Momentum Compaction -	$\alpha$	.032
Synchrotron Frequency	$\omega$	6490kHz
Electron Bunch length	$\sigma$	200psec
Energy Damping Time	$\tau$	65msec
Electron Beam Width (Horz.)	$\sigma_x$	.34mm
Electron Beam Width (Vert.)	$\sigma_y$	.33mm
Undulator Period	$\lambda_u$	7.78cm
Undulator K Value	K	1.93
Number of Periods	N	17
Laser Wavelength	$\lambda$	5145A
laser Peak Intensity	I	175watts/cm <sup>2</sup>
Laser Beam Waist	w	1.2mm
Orbit Frequency	$\omega_0$	13.618MHz
Detection Frequency	$\omega_d$	1062.2MHz (78th harmonic)
Number of Bunches		1

#### FIGURE CAPTIONS

Figure 1: Schematic of the bunch lengthening experiment

Figure 2: Time averaged response of the electron bunch length at low current. The upper trace shows the time dependence of  $\log F(\omega)$ , the power output of the photodiode detector at the 1062.2 MHz harmonic of the orbit frequency. As described in the text, an increase in the bunch length reduces the amplitude of  $\log F(\omega)$ . The lower trace records the laser intensity incident on the electron beam.

Figure 3: a) Bunch lengthening as a function of undulator gap. The maximum signal corresponds to a bunch lengthening of 6% occurring at a gap of 43.3mm or equivalently  $K = 1.93$ .  
b) Spontaneous emission of the permanent magnet undulator as a function of undulator gap at fixed frequency (5145Å)  
c) Theoretical bunch lengthening as a function of undulator gap. The divisions indicated on all three curves corresponds to 1mm change in undulator pole face gap.

Figure 4: Time averaged response of electron bunch length to an externally chopped laser in the anomalous bunch lengthening regime. The upper trace in all three photographs shows the response of  $\log F(\omega)$  (increasing bunch length downward) to the chopped external laser beam recorded in the lower trace of each photograph. a) 2.5mA average current, RF Voltage of 4.0kV, and chopping period of 107msec. b) 2mA, 5.76kV, and a chopping period of 107msec. c) 2.5mA average current, 12.0kV RF, and a chopping period of 560msec (only the laser 'on' portion is shown).

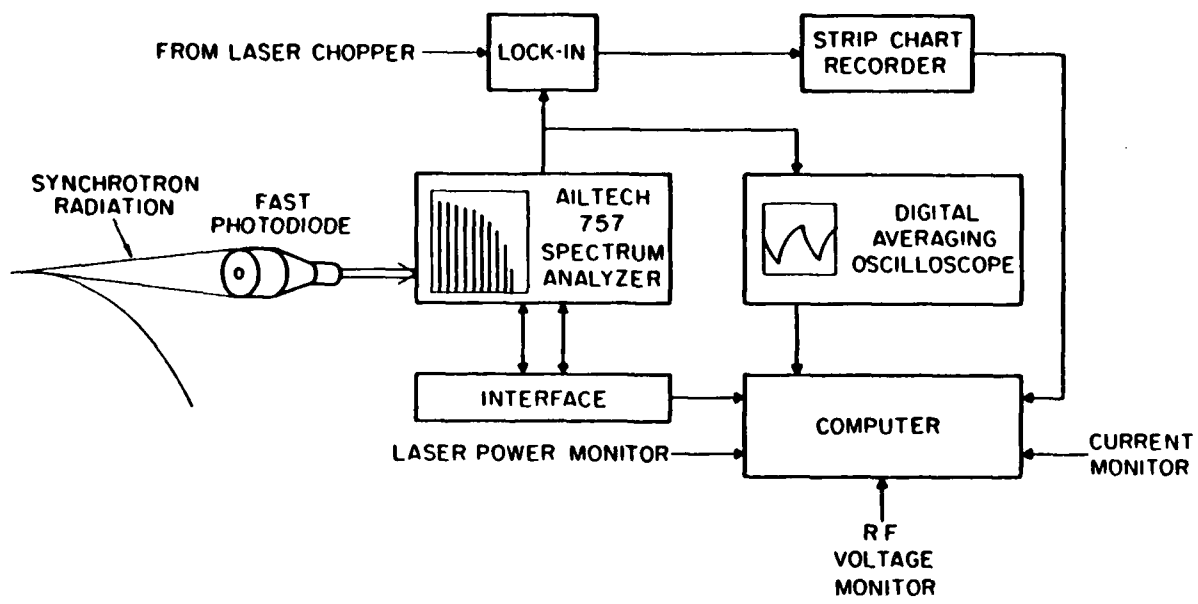


Figure 1

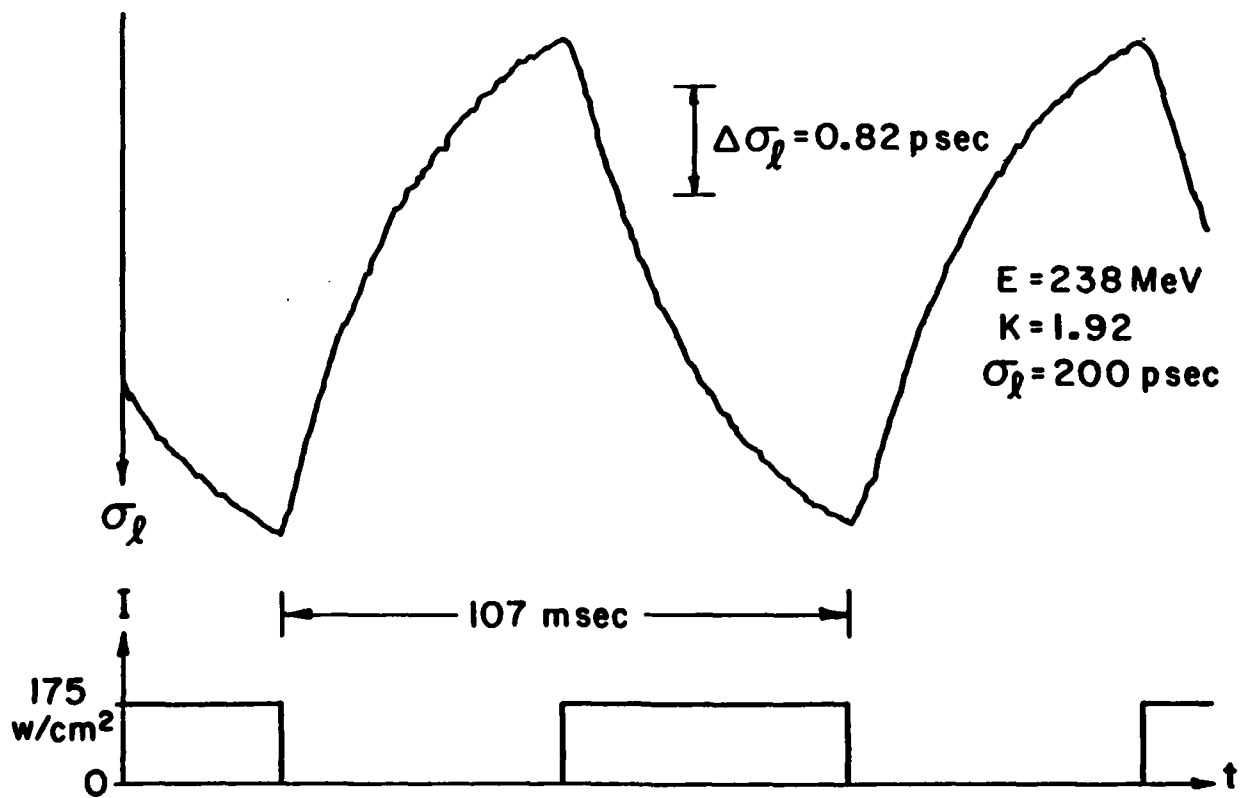
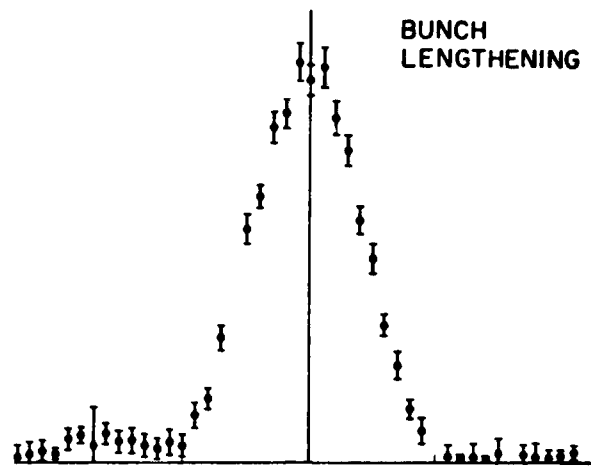
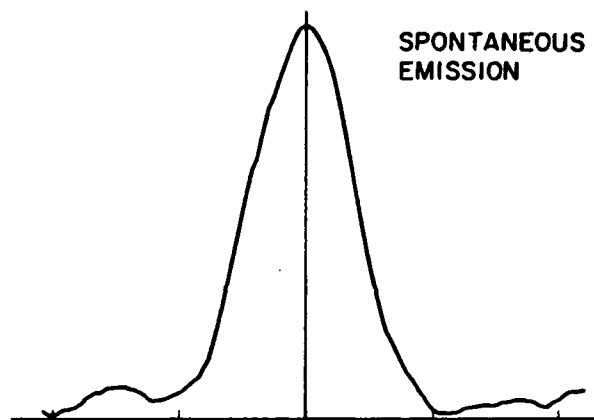


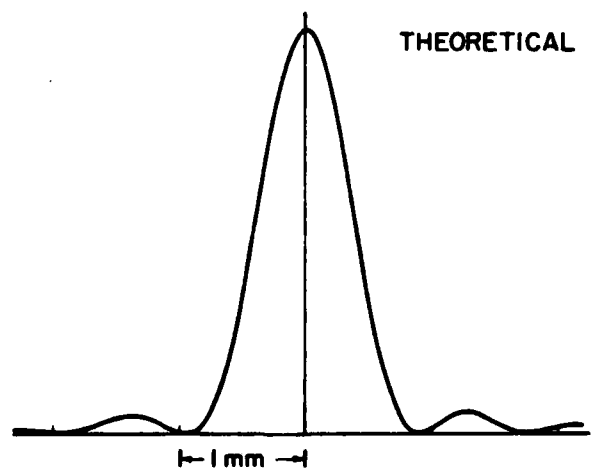
Figure 2



(a)



(b)



(c)

Figure 3

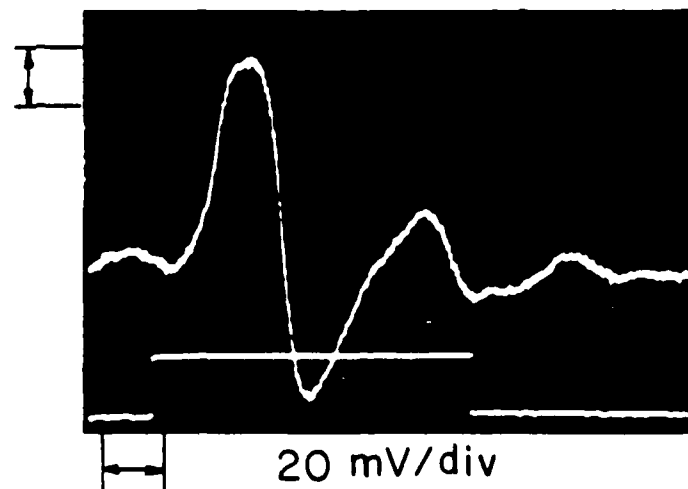
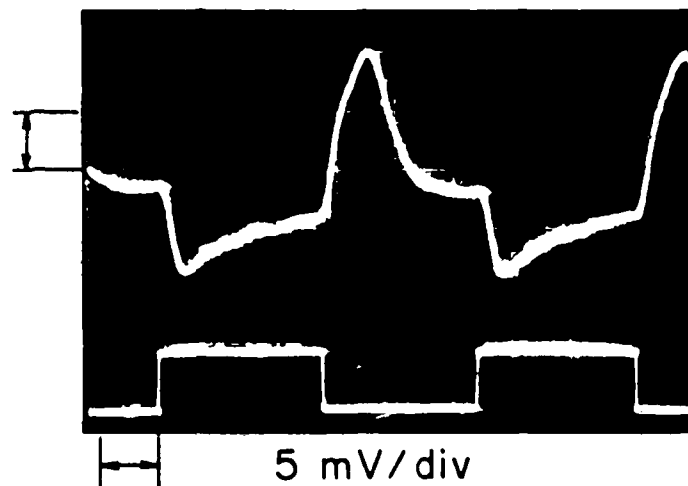
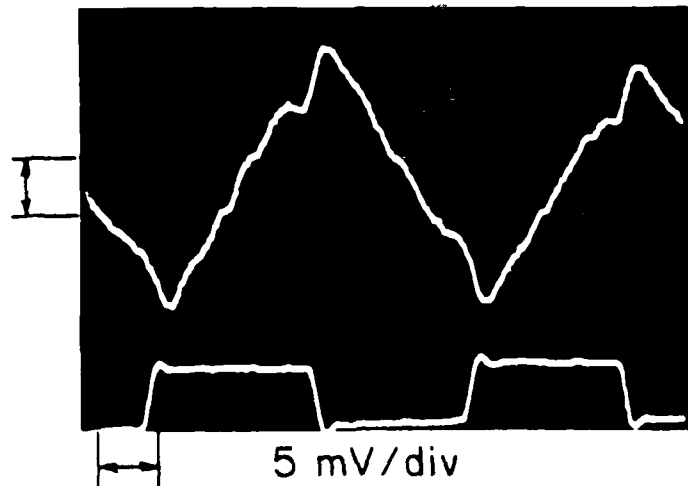


Figure 4

END

DATE  
FILMED

3 - 83

DTIC